

Structural Behavior of Alcohol–1,4-Dioxane Mixtures through Dielectric Properties Using TDR

Ashok C. Kumbharkhane* and M. N. Shinde

School of Physical Sciences, Swami Ramanand Teerth Marathwada University, Nanded-431 606, India

Suresh C. Mehrotra

Department of Computer Science & Information Technology, Dr. Babasaheb Ambedkar Marathwada University, Aurangabad-431 004, India

Noriaki Oshiki, Naoki Shinyashiki, and Shin Yagihara

Department of Physics, Tokai University, Kanagawa 259-1292, Japan

Seiichi Sudo

Department of Physics, Tokyo City University, Tamazutsumi, Setagaya, Tokyo 158-8557, Japan

Received: May 25, 2009; Revised Manuscript Received: July 30, 2009

The values of complex permittivity for alcohol–1,4-dioxane (DX) mixtures with various concentrations have been determined in the frequency range 10 MHz to 20 GHz using the time domain reflectometry (TDR) method. Numbers of hydrogen bonds between alcohol–alcohol and alcohol–dioxane pairs are estimated from the values of the static dielectric constant by using the Luzar model. The model provides a satisfactory explanation of the experimental results related to the static dielectric constant. The binding energies for alcohol–alcohol (pair 11) and alcohol–DX (pair 12) are estimated to be -13.98 and -16.25 kJ/mol, respectively. The results have also been compared with previous results of the ethyleneglycol–DX system.

Introduction

Over the past few years, extensive experimental and theoretical studies concerning the dielectric behavior of alcohols have been reported.^{1–11} The main thrusts of these studies were to understand (a) the structure of polar liquids in terms of hydrogen bonding and (b) modification of hydrogen bonding due to the presence of other polar or nonpolar molecules. Hydrogen bonding is a complex phenomenon in the liquid state due to uncertainty in identifying the particular bonds and the number of molecules involved. The local structures of hydrogen-bonding liquids are complicated due to molecular clusters and network structures through hydrogen bonds. The importance of hydrogen bonding as a force governing the structure and dynamics of chemical and biological systems has been pointed out in a plethora of papers.^{1–16}

The dielectric properties have been studied as a function of $-OH$ group and number of carbon atoms in alcohol in order to understand the significance of hydrogen-bond interaction in alcohol.^{1–11} The study of the dielectric properties of alcohols on addition of nonpolar solute (like dioxane) provides information about breaking of the molecular multimer structures in the systems. The dipole moment of dioxane is very small ($\mu = 0.45$ D). Mixtures of alcohol–1,4-dioxane (DX) have been extensively studied by dielectric spectroscopic techniques. The relaxation process is explained by a microscopic heterogeneous structure based on three kinds of pairs formed in the mixtures. Pair 1 is formed due to interaction between alcohol molecules (solute–solute). Pair 2 is due to interaction between dioxane and alcohol molecules (solvent–solute). Pair 3, which formation of this is not probable due to the nonpolar structure, is due to

interaction between two dioxane molecules (solvent–solvent). However, the structure for the alcohol–dioxane mixtures is complex and is not clear yet. In our earlier work,¹¹ we have reported results of dielectric relaxation measurements for ethyleneglycol–1,4-dioxane mixtures with various concentrations by using the time domain reflectometry (TDR) method in the frequency range 100 MHz to 20 GHz. The concentration dependence of the population of two kinds of cooperative domains for the ethyleneglycol–1,4-dioxane mixtures was also discussed. In a dioxane–alcohol mixture with a value of 0.8, the average size of ethyleneglycol–1,4-dioxane and the average number of hydrogen bonds between ethyleneglycol and 1,4-dioxane molecules are found to be maximum. It seems that one ethyleneglycol molecule bonds with about two 1,4-dioxane molecules at this concentration.

In the present work, a study related to dielectric measurements of the mixtures of 1,4-dioxane (DX) and aliphatic alcohols using the TDR method is reported. The aliphatic alcohols used in the present study are 1-propanol, 2-propanol, 1,2-propanediol, and 1,3-propanediol. These mixtures form interesting systems because all of these alcohols have three carbon atoms, whereas the number of hydroxyl groups and their position in the structures are different. The experimental results of static dielectric constants have been used to estimate the numbers of pairs 1 and 2 formed in mixtures. This provides molecular parameters related to solute–solvent interaction. These are also compared with earlier reported work.¹¹

Experiments

The alcohols used in these experiments are 1-propanol (1PrOH), 2-propanol (2PrOH), 1,2-propyleneglycol (12PG), and

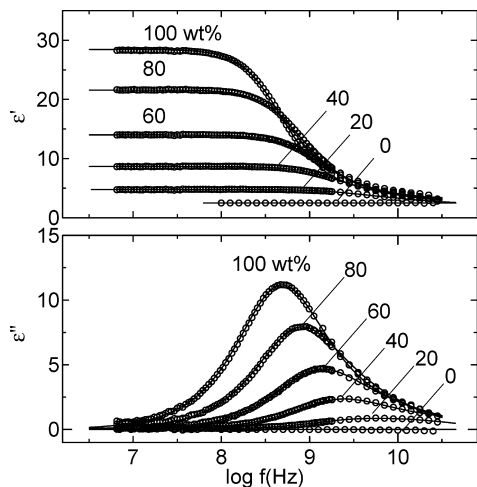


Figure 1. Frequency dependences of the dielectric constant and loss for 1,2-propyleneglycol–1,4-dioxane mixtures at various concentrations at 25 °C. The solid lines were calculated from the sum of the KWW and Debye equations.

1,3-propyleneglycol (13PG). All have been purchased from Aldrich. The mixtures of these alcohols and 1,4-dioxane were prepared with concentrations ranging from 100 to 0 wt % in the interval of 10% by weight. The complex permittivity of the mixtures was determined in the frequency range 10 MHz to 20 GHz at 25 °C. In order to cover the wide frequency range from 10 MHz to 20 GHz, we used two dielectric measurement systems. From 1 to 20 GHz, a time domain reflectometry (TDR) method was employed,^{17,18} and an RF impedance/material analyzer (HP 4291A) was used for the frequency range 10 MHz to 1.8 GHz.

Results

The values of the permittivity parameters for alcohol–DX mixtures as a function of frequency are shown in Figure 1 for 12PG–DX mixtures with various values of concentration (0, 20, 40, 60, 80, and 100 wt % 12PG) at 25 °C. A peak in the plot of the imaginary part of permittivity vs frequency is observed in the entire concentration range. It can be seen from Figure 1 that the position of the peak shifts toward lower frequency with increasing alcohol concentration. This shows that the relaxation time decreases with an increase of alcohol in the mixture.

We performed a curve-fitting procedure for the dielectric spectrum of the alcohol–DX mixture, in order to determine the dielectric relaxation parameters. In general, the dielectric loss spectrum of the polyalcohol is an asymmetric shape, and it is described by the Kohlrausch–Williams–Watts (KWW) equation or the Havriliak–Negami equation.^{19–22} Recently, dielectric measurements up to the sub-THz and THz regions have been performed for water, monohydric alcohol, ethyleneglycol, and alcohol–water mixtures around room temperature, and some relaxation processes have been observed in the frequency range higher than the observed loss-peak frequency.^{23–26} The amplitudes of these high-frequency processes are much lower than that of the primary process, and the relaxation times are 1–2 decades smaller than that of the primary process. Then, the loss peak of these high-frequency processes is hidden by the primary process, and these processes behave as a high-frequency wing of the primary process. Therefore, the dielectric spectrum of the alcohol–DX mixtures is simulated in a satisfactory manner by the simple summation of the KWW and Debye equations as follows:

$$\varepsilon^*(\omega) = \varepsilon_\infty + \Delta\varepsilon_1 \int_0^\infty \left[-\frac{d\Phi(t)}{dt} \right] \exp(-j\omega t) dt + \frac{\Delta\varepsilon_h}{1 + j\omega\tau_h} \quad (1)$$

Here,

$$\Phi(t) = \exp\left[-\left(\frac{t}{\tau_1}\right)^{\beta_K}\right] \quad (2)$$

where $\Delta\varepsilon$ is the relaxation strength, which is in proportion to the dielectric susceptibility. τ is the relaxation time, which is the time constant of the relaxation. ε_∞ is the limiting high-frequency permittivity, ω is the angular frequency, and β_K ($0 < \beta_K \leq 1$) is a parameter for the asymmetrical broadness of the loss peak. The subscripts in eq 1 indicate the KWW-type low (l)- and Debye-type high (h)-frequency processes. The static dielectric constant is written as $\varepsilon_0 = \Delta\varepsilon_l + \Delta\varepsilon_h + \varepsilon_\infty$. As an example of the results of the curve fitting, Figure 2 shows the loss spectrum of the 60 wt % 12PG–DX mixtures. The relaxation curve calculated from the curve fitting procedure is in good agreement with the experimental results in the entire frequency range measured.

Figure 3 shows a plot of the dielectric relaxation time as a function of the mole fraction of DX, x_{DX} , for the alcohol–DX mixtures. The dielectric relaxation time of the low-frequency process decreases with increasing x_{DX} , and it does not depend linearly on x_{DX} . The relaxation time of the high-frequency process slightly decreases with increasing x_{DX} .

Figure 4 shows a plot of the dielectric relaxation strength as a function of the mole fraction of DX, x_{DX} , for the alcohol–DX mixtures. The relaxation strength of the low-frequency process decreases with increasing x_{DX} . It can be seen from the plot that the relaxation strength of the high-frequency process is independent of x_{DX} for $x_{DX} < 0.6$ and decreases with increasing x_{DX} for $x_{DX} > 0.6$.

Discussion

The significance of hydrogen bonds to the dielectric properties of the mixture can be studied using the Luzar model.²⁷ It is based on the statistical behavior of solute–solvent interaction assuming that only solute–solute and solute–solvent pairs are formed in the mixture. Thus, it is applicable for a polar–nonpolar mixture. The model is successfully applied to a water–dimethylsulfoxide (DMSO) system.²⁷ We have used the same model to explain the static dielectric permittivity of the mixture. The static dielectric permittivity in terms of the Kirkwood correlation factor “ g_i ” for a mixture can be expressed as follows²⁷

$$[(\varepsilon_{0i} - \varepsilon_{\infty i})(2\varepsilon_{0i} + \varepsilon_{\infty i})/9\varepsilon_{0i}] = 4\pi/9kT \sum_{i=1}^2 g_i \rho_i \mu_i^2 \quad (3)$$

where $i = 1$ and 2 represent alcohol and dioxane, respectively; μ_i is the corresponding dipole moment in the gas phase, ρ_i is the density, k is the Boltzmann constant, T is the temperature, an ε_{0i} and $\varepsilon_{\infty i}$ are the static dielectric constant and dielectric constant at high frequency. g_i is the Kirkwood correlation factor for the i th liquid system. The Kirkwood correlation factor “ g ” is a parameter affording information regarding the orientation of electric dipoles in polar liquids. The correlation factors g_1 and g_2 were computed using the Luzar model by considering

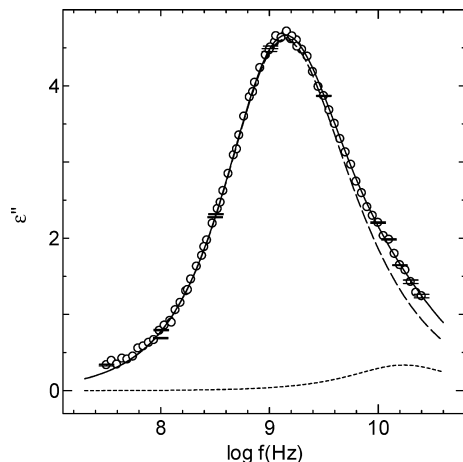


Figure 2. Dielectric loss spectrum of 60 wt % 1,2-propyleneglycol-1,4-dioxane at 25 °C. The dashed and dotted lines were calculated from the KWW and Debye equations, respectively. The solid line was calculated from the sum of the KWW and Debye equations.

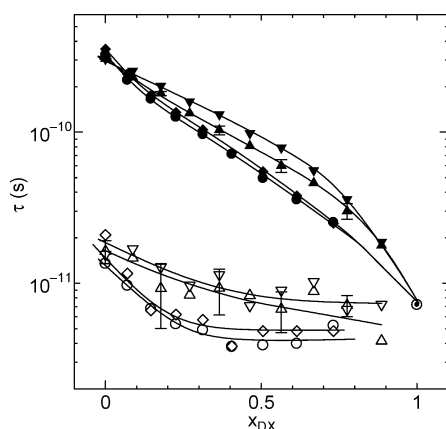


Figure 3. Mole fraction of 1,4-dioxane dependence of the relaxation time. Closed and open circles indicate the low- and high-frequency processes, respectively. ●, 1-propanol; ◆, 2-propanol; ▲, 1,2-propyleneglycol; ▼, 1,3-propyleneglycol.

only the hydrogen-bond contribution to the dipole-dipole correlation and are described by the relation²⁷

$$g_1 = 1 + Z_{11} \cos \varphi_{11} + Z_{12} \cos \varphi_{12} (\mu_2/\mu_1) \quad (4)$$

$$g_2 = 1 + Z_{21} \cos \varphi_{21} (\mu_1/\mu_2) \quad (5)$$

where $Z_{11} = 2\langle n_{\text{HB}}^{11} \rangle$, $Z_{12} = 2\langle n_{\text{HB}}^{12} \rangle$, and $Z_{21} = 2\langle n_{\text{HB}}^{21} \rangle V_2 / (1 - V_2)$ are the average number of particles forming the hydrogen bond with alcohol-alcohol and alcohol-dioxane pairs, respectively. V_2 is the mole fraction of alcohol. φ_{11} and φ_{21} are the angles between the neighboring dipoles of alcohol and dioxane molecules. The values of g_1 and g_2 for different alcohol-DX mixtures are computed by using the parameters given in Table 1 and are shown in Figure 5. The values of g_1 and g_2 depend on the concentration of DX in alcohol-DX mixtures.

The average number of hydrogen bonds $\langle n_{\text{HB}}^{11} \rangle$, $\langle n_{\text{HB}}^{12} \rangle$, and $\langle n_{\text{HB}}^{21} \rangle$ per alcohol molecule for $1i$ pairs ($i = 1, 2$) has been determined according to the following relation²⁷

$$\langle n_{\text{HB}}^{1i} \rangle = n_{1i} \omega_{1i} / n_1 \quad (6)$$

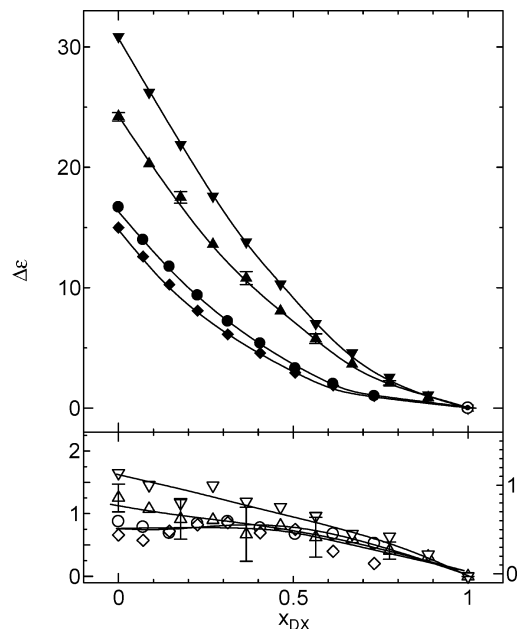


Figure 4. Mole fraction of 1,4-dioxane dependence of the relaxation strength. Closed and open circles indicate the low- and high-frequency processes, respectively. ●, 1-propanol; ◆, 2-propanol; ▲, 1,2-propyleneglycol; ▼, 1,3-propyleneglycol.

TABLE 1: Molecular Parameters Used in Computation of the Static Dielectric Constants

molecular parameter	1PrOH	2PrOH	12PG	13PG
dipole moment of alcohol in debyes, μ_1	2.26D	2.20D	2.65D	2.95D
dipole moment of DX in debyes, μ_2	0.97D	0.97D	0.97D	0.97D
polarizability for alcohol in \AA^3	4.94	4.94	4.94	4.94
polarizability for DX in \AA^3	2.80	2.80	2.80	2.80
binding energy for alcohol-alcohol (E^{11}) (kJ/mol)	-13.98	-13.98	-13.98	-13.98
binding energy for alcohol-DX (E^{12}) (kJ/mol)	-16.25	-16.25	-16.25	-16.25

where $\omega^{1i} = 1/(1 + \alpha^{1i} e^{-\beta E^{1i}})$ is the probability of bond formation between alcohol and 1,4-dioxane. n_1 is the number density of 1,4-dioxane molecules. The value of $\beta = 1/kT$ and

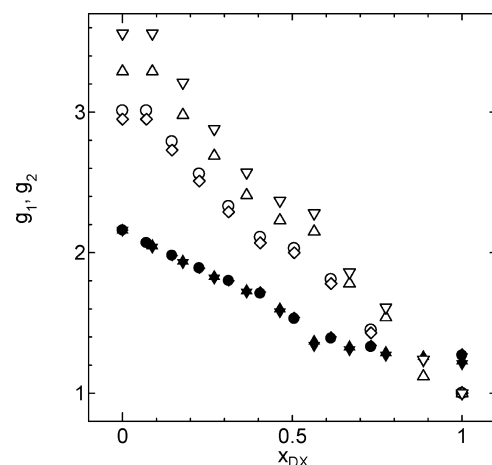


Figure 5. Mole fraction of 1,4-dioxane dependence of the g_1 (closed symbols) and g_2 (open symbols): ●, 1-propanol; ◆, 2-propanol; ▲, 1,2-propanediol; ▼, 1,3-propanediol.

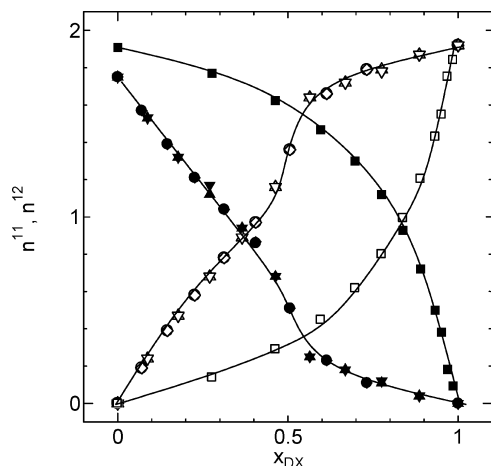


Figure 6. Mole fraction of 1,4-dioxane dependence of the n^{11} (closed symbols) and n^{12} (open symbols): ●, 1-propanol; ◆, 2-propanol; ▲, 1,2-propanediol; ▼, 1,3-propanediol; □, ethyleneglycol.

α^{li} is the ratio of the two sub volume of the phase space, related to the non-hydrogen-bonded and hydrogen-bonded pairs. These hydrogen-bonded pairs have only two energy levels, E^{11} and E^{12} , for alcohol–alcohol and alcohol–dioxane pair formed bonds, respectively. The values of $\langle n_{\text{HB}}^{11} \rangle$ and $\langle n_{\text{HB}}^{12} \rangle$ depend on the densities of the hydrogen-bonding pairs between alcohol–1,4-dioxane n^{12} and those between alcohol–alcohol molecule, i.e., $n^{11} = 2n_1 - n^{12}$. This can be calculated when alcohol–alcohol (pair 1) and alcohol–1,4-dioxane (pair 2) are formed.²⁷ Figure 6 shows a plot of the average number of hydrogen bonds between alcohol–alcohol molecules (11 pairs) and alcohol–1,4-dioxane (12 pairs) against the mole fraction of 1,4-dioxane. It can be seen from the values that $\langle n_{\text{HB}}^{11} \rangle$ and $\langle n_{\text{HB}}^{12} \rangle$ depend on the concentration of DX in alcohol–DX mixtures.

The average number of hydrogen-bonded alcohol–alcohol, $[n_{\text{HB}}^{11}]_V$, and alcohol–DX, $[n_{\text{HB}}^{12}]_V$, per unit volume (cm^3) are computed as follows:¹¹

$$[n_{\text{HB}}^{11}]_V = \frac{C_A \rho_{\text{mix}} N_A n_{\text{OH}} n_{\text{HB}}^{11}}{M_A} \quad (\text{/cm}^3)$$

and

$$[n_{\text{HB}}^{12}]_V = \frac{C_A \rho_{\text{mix}} N_A n_{\text{OH}} n_{\text{HB}}^{12}}{M_{\text{DX}}} \quad (\text{/cm}^3) \quad (7)$$

Here, C_A is the weight fraction of alcohol, ρ_{mix} (g/cm^3) is the density of the mixtures, N_A is the Avogadro number as 6.02×10^{23} (/mol), n_{OH} is the number of OH groups in a molecule, and M_A and M_{DX} are the molecular weight of alcohol and DX molecules, respectively. Figure 7 shows plots of $[n_{\text{HB}}^{11}]_V$ and $[n_{\text{HB}}^{12}]_V$ vs x_{DX} . The value of $[n_{\text{HB}}^{11}]_V$ decreases linearly with increasing x_{DX} , up to $x_{\text{DX}} = 0.7$, and it appears to change the slope at $x_{\text{DX}} = 0.7$, tending to zero. The value of $[n_{\text{HB}}^{12}]_V$ has a maximum at $x_{\text{DX}} \approx 0.7$ in the alcohol–DX mixture. These results provide information regarding the interaction of the alcohol–alcohol and alcohol–DX molecules.

The concentration dependence of the dielectric permittivity is calculated using eqs 3–6 and is compared with experimental data. The model gives a good qualitative account of the dielectric permittivity of the alcohol–1,4-dioxane mixtures. In our analysis, the best possible values of molecular

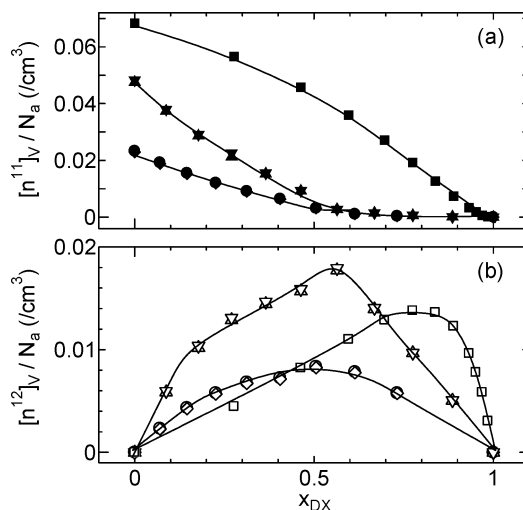


Figure 7. Mole fraction of the 1,4-dioxane dependence of the number of hydrogen bonds per unit volume (a) n^{11}/N_A (closed symbols) and (b) n^{12}/N_A (open symbols): ●, 1-propanol; ◆, 2-propanol; ▲, 1,2-propanediol; ▼, 1,3-propanediol; □, ethyleneglycol.

parameters with which the theoretical dielectric permittivity values are in agreement with experimental values are shown in Table 1. All parameters used in the calculations are the same as those given in ref 27. The dipole moment arrangement around one OH group is independent of the number and position of OH groups in polar molecules from the results of n^{11} and n^{12} but strongly depends on the number of carbon atoms, as shown in Figures 6 and 7. These results indicate that the hydrogen bonding in the alcohol–DX mixtures is satisfied by the carbon atoms of the alcohol molecules.

In previous work, we discussed the cooperative region in which the reorientation of molecules cooperatively occurs by hydrogen bonding for the ethyleneglycol–DX mixtures.¹¹ The relaxation time is related to the apparent activation free energy of the rearrangement of dipoles by the Eyring formula²⁸

$$\tau = \frac{h}{k_B T} \exp\left(\frac{\Delta G}{RT}\right) \quad (8)$$

Here, h is the Planck constant, k_B is the Boltzmann constant, T is the absolute temperature, R is the gas constant, and ΔG is the apparent activation free energy, which relates to the relaxation rate in the molecular environment. When the alcohol–DX mixture can be treated as the ideal mixture, the free energy of the mixed environment is equal to the arithmetical mean of the free energies of the pure liquids, and the apparent activation free energy, ΔG_{mix} , is given by²⁹

$$\Delta G_{\text{mix}} = x_{\text{DX}} \Delta G_{\text{DX}} + (1 - x_{\text{DX}}) \Delta G_A \quad (9)$$

where ΔG_{DX} and ΔG_A are the apparent activation free energies for pure DX and alcohol, respectively. Then, the relaxation time in the ideal case, τ_{ideal} , for the mixture is given by

$$\tau_{\text{ideal}} = \frac{h}{kT} \exp\left(\frac{\Delta G_{\text{mix}}}{RT}\right) = \tau_{\text{DX}}^{x_{\text{DX}}} \tau_A^{(1-x_{\text{DX}})} \quad (10)$$

where τ_{DX} and τ_A are the relaxation time for pure DX and alcohol, respectively. This equation gives a linear dependence of the plots of the logarithm of τ_{ideal} vs x_{DX} . In our results,

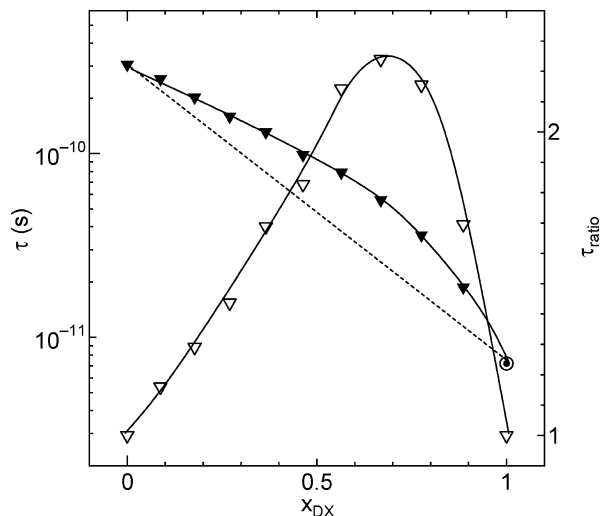


Figure 8. Mole fraction of 1,4-dioxane dependence of the relaxation time for 1,3-propanediol–1,4-dioxane. Open symbols indicate the ratio of the observed relaxation time to the relaxation time of the ideal mixtures.

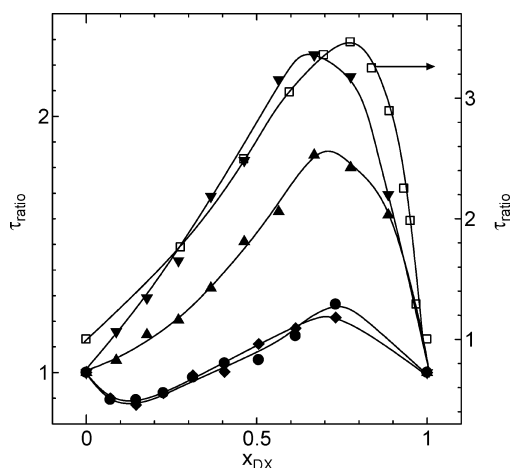


Figure 9. Mole fraction of the 1,4-dioxane dependence of the τ_{ratio} : ●, 1-propanol; ◆, 2-propanol; ▲, 1,2-propanediol; ▼, 1,3-propanediol; □, ethyleneglycol.¹¹

as shown in Figure 3, the observed relaxation time of the three carbon atoms in alcohol–DX mixtures (τ_{obs}) deviates from τ_{ideal} in the entire concentration range. τ_{ratio} is defined as the ratio $\tau_{\text{obs}}/\tau_{\text{ideal}}$ to discuss the deviation of τ_{obs} from τ_{ideal} , as shown in Figure 8. This value reflects the deviation from the ideal case, i.e., the contribution of the cooperative region of the alcohol and DX molecules by hydrogen bonds.

Figure 9 shows the plots of τ_{ratio} against x_{DX} for the alcohol–DX mixtures. The value of τ_{ratio} clearly shows a maximum at $x_{\text{DX}} \cong 0.7$ in 12PD–DX and 13PD–DX mixtures. In the case of 1PrOH–DX and 2PrOH–DX mixtures, it is seen that the value of τ_{ratio} also shows a maximum around $x_{\text{DX}} \cong 0.7$. This concentration agrees well with the concentration at which $[n_{\text{HB}}^2]_{\text{V}}$ shows a maximum. These results indicate that $[n_{\text{HB}}^2]_{\text{V}}$ increases with increasing x_{DX} , when DX is added in the pure alcohol. At $x_{\text{DX}} \cong 0.7$, $[n_{\text{HB}}^2]_{\text{V}}$ reaches a maximum, and the size of the cooperative region of the alcohol–DX molecules shows the maximum. It is noted that the maximum of the τ_{ratio} , $[\tau_{\text{ratio}}]_{\text{max}}$, of 12PG–DX and 13PG–DX mixtures is larger than that of the 1PrOH–DX and 2PrOH–DX mixtures, and $[\tau_{\text{ratio}}]_{\text{max}}$ of the alcohol–DX mixtures with three carbon atoms is

smaller than that of the ethyleneglycol–DX mixtures, as shown in Figure 9. These results indicated that two OH groups in 12PG and 13PG molecules can interact independently with DX molecules, and the size of the cooperative region for the 12PG and 13PG mixtures is larger than that for 1PrOH–DX and 2PrOH–DX mixtures. The cooperativity of the alcohol and DX molecules strongly depends on the number of carbons, and the size of the cooperative region of alcohol–DX mixtures with three carbon atoms is smaller than that of the ethyleneglycol–DX mixture.

Conclusion

The concentration dependent loss vs frequency plot reveals a peak which shifts toward lower frequency with increase of alcohol in the mixtures. The permittivity spectra can well be described by summation of the Kohlrausch–Williams–Watts (KWW) and Debye equations. The mixtures contain two types of hydrogen bonds, one with alcohol–alcohol and the other with alcohol–DX. The Luzar model indicates that the bonding energy of the second pair is found to be 16% smaller than the corresponding value of the first pair. This value was 6% for the ethyleneglycol (EG)–DX system. The number of hydrogen-bonded second pair in the mixture is maximum at $x_{\text{DX}} = 0.7$, whereas this value was 0.8 for EG–DX mixture. The hydrogen-bond density between the alcohol and DX molecules depends on not only the number OH groups in polar molecules but also the number of carbons.

Acknowledgment. This work was partly supported by the Ministry of Education, Science, Sports and Culture, Grant-in-Aid for specially promoted Research (18031034). The financial support from the Department of Science & Technology (DST), New Delhi, India, is also gratefully acknowledged.

References and Notes

- Hanna, F. F.; Gestblom, Bo.; Soliman, A. *Phys. Chem. Chem. Phys.* **2000**, *2*, 5071.
- Tabellout, M.; Lancelour, Emery, J. R.; Hayward; Pethrick, *J. Chem. Soc., Faraday Trans.* **1990**, *86*, 1493.
- Bertolini, D.; Casstari, M.; Salvetti, G. *J. Chem. Phys.* **1983**, *78*, 365.
- Perl, J. P.; Wassan, D. T.; Winsor, I. V.; Cole, R. H. *J. Mol. Liq.* **1984**, *28*, 103.
- Sengwa, R. J.; Sankhla, S.; Shinyashiki, N. *J. Solution Chem.* **2008**, *37*, 137–153.
- Gestblom, B.; Sjoblom, J. *Acta Chem. Scand., Ser. A* **1984**, *38*, 47.
- Kumbharkhane, A. C.; Puranik, S. M.; Mehrotra, S. C. *J. Chem. Soc., Faraday Trans.* **1991**, *87* (10), 1569.
- Yagihara, S.; Nozaki, R.; Mashimo, S.; Higasi, K. *Chem. Lett.* **1985**, *1*, 137.
- Mashimo, S.; Miura, N.; Umehara, T.; Yagihara, S.; Higasi, K. *J. Chem. Phys.* **1992**, *96*, 6358.
- Kanse, K. S.; Chavan, S. D.; Kumbharkhane, A. C.; Mehrotra, S. C. *J. Polym. Mater.* **2006**, *23* (1), 47.
- Sudo, S.; Oshiki, N.; Shinyashiki, N.; Yagihara, S.; Kumbharkhane, A. C.; Mehrotra, S. C. *J. Phys. Chem. A* **2007**, *111* (16), 2993.
- Petong, P.; Pottel, R.; Kaatze, U. *J. Phys. Chem. A* **2000**, *104*, 7420.
- Petong, P.; Pottel, R.; Kaatze, U. *J. Phys. Chem. A* **1999**, *103*, 6114.
- Saize, L.; Padro, J. A.; Guardia, E. *J. Chem. Phys.* **2001**, *114*, 3187.
- Bako, T.; Grosz, G.; Palinkas, M. C.; Bellissent, F. *J. Chem. Phys.* **2003**, *118*, 3215.
- Tominaga, Y.; Takeuchi, S. M. *J. Chem. Phys.* **1996**, *104*, 7377.
- Mashimo, S.; Umehara, T.; Redlin, H. *J. Chem. Phys.* **1991**, *95*, 6257.
- Mashimo, S.; Kuwabara, S.; Yagihara, S.; Higasi, K. *J. Chem. Phys.* **1989**, *90*, 3292.
- Kohlrausch, R. *Prog. Ann. Phys.* **1854**, *91*, 179.
- Williams, G.; Watts, D. C. *Trans. Faraday Soc.* **1971**, *66*, 80.
- Havriliak, S.; Negami, S. *Polymer* **1963**, *8*, 9874.
- Kremer, F.; Schönhal, A. *Broadband Dielectric Spectroscopy*; Springer: New York, 2002.

- (23) Garg, K. S.; Smyth, C. P. *J. Phys. Chem.* **1965**, *69*, 1294.
(24) Barthel, J.; Bachhuber, K.; Buchner, R.; Hetzenauer, H. *Chem. Phys. Lett.* **1990**, *165*, 369.
(25) Kaatze, U.; Behrends, R.; Pottel, R. *J. Non-Cryst. Solids* **2002**, *305*, 19.
(26) Fukasawa, T.; Sato, T.; Watanabe, J.; Hama, Y.; Kunz, W.; Buchner, R. *Phys. Rev. Lett.* **2005**, *95*, 197802.

- (27) Luzar, A. *J. Mol. Liq.* **1990**, *46*, 221.
(28) Hill, N. E.; Vaughan, W. E.; Price, A. H.; Davies, M. *Dielectric Properties and Molecular Behaviour*; Reinhold: London, 1969.
(29) Bertolini, D.; Cassettari, M.; Ferrari, C.; Tombari, E. *J. Chem. Phys.* **1998**, *108*, 6416.

JP904845P